Biophysical Chemistry 4 (1976) 349–362

THE ELECTROPHORETIC HEMOLYTIC PLAQUE ASSAY – THEORY ☆

Byron GOLDSTEIN ‡ and Alan S. PERELSON
Theoretical Division, University of California, Los Alamos Scientific Laboratory, Los Alamos, New Mexico 87544, USA.

Received 30 March 1976

We use the mathematical theory of plaque growth to determine if there is merit in performing a hemolytic plaque assay in the presence of an external electric field. In particular, we study the effects of an electric field on the transport of antibodies secreted by a single lymphocyte and on the size and shape of the plaques they produce. Our results indicate that in the presence of an applied electric field: (1) The mobility of the antibodies produced by the antibody forming cell can be determined from the plaque shape. (In the electric field the plaques are no longer circular, but cigar shaped.) (2) By changing the magnitude or direction of the applied electric field more than one plaque can be generated by a single AFC. Thus changes in mobility or the rate of antibody secretion can be assayed. (3) Plaques will reach a steady state size; for good emitters (cells that secrete antibodies at a high rate or that secrete high affinity antibodies) this steady state will be achieved rapidly.

Equations are given which describe both the temporal development and steady state plaque size and shape. From the equations, computer generated plots of plaques produced by typical antibody forming cells are presented. These plots are then used to show how pictures of plaques formed in an electric field can be analyzed to determine the antibody mobility.

1. Introduction

Since the introduction of the hemolytic plaque assay for the detection of single antibody-forming cells (AFC) (Jerne and Nordin [1], Jerne et al. [2]), a great deal of effort has gone into improving the technique (see, for example refs. [3–5]). A major improvement in sensitivity was achieved through the introduction of monolayer techniques. Both the liquid monolayer technique [6,7] and the monolayer techniques which use support material [5,8–10] have received wide use.

In this paper we point out the advantages of performing the direct hemolytic plaque assay in the presence of an electric field. We use the recently developed mathematical theory of hemolytic plaque growth [3, 11–13], to study the effects of an electric field on the temporal and spatial development of plaques. From the theory we conclude that in the presence of an electric field, the plaque technique becomes capable of yielding more information than the presently used plaque assays.

First recall the properties of plaque growth when there is no electric field present. Consider an AFC which is placed in a thin layer at time $T = 0$. The layer contains red blood cells (RBC) and complement so that plaque growth can be monitored continuously. Assume the AFC begins emitting IgM antibodies at time $T = T_0$ and emits them at a constant rate for the remainder of the experiment. For times less than T_0 there is of course no plaque, while for times greater than T_0 a circular plaque develops whose radius, R, increases with time in the following way:

$$R^2 = k(T - T_0). \tag{1}$$

For a given plaque k is a constant.

The growth of the plaque radius as described by eq. (1) has been observed in direct plaque experiments [8,14,15] and has been predicted by theory [12,13]. The theory shows that this result occurs only when there is local equilibrium between the bound and free antibodies at the plaque radius. In this case only the equilibrium constant enters the theory rather than the

☆ Work performed under the auspices of the U.S. Energy Research Development Administration.
‡ Permanent Address: Department of Physics, Fairleigh Dickinson University, Teaneck, New Jersey 07666.

the various rate constants which are needed to describe the detailed kinetics of IgM–RBC binding. This theoretical result is reviewed in Appendix 1.

As long as an AFC produces antibodies at a constant rate and is in a thin layer, its plaque will continue to grow. As can be seen from eq. (1), the plaque radius does not approach a limiting value. However, in the presence of an electric field the plaque does approach a final size. Further, for reasonable values of the electric field (10 V/cm or less), the time to reach the final size may be quite short (20 min or less). Normally the speed of plaque growth is limited by diffusion, but in an electric field there is a rapid transport of antibodies away from the AFC. If the AFC is a "good emitter", by which we mean if it secretes high affinity antibodies or secretes moderate to low affinity antibodies rapidly, this transport speeds up plaque growth. However, if the AFC is a "poor emitter", i.e., if it secretes slowly or if it secretes low affinity antibodies, then the electric field may spread these antibodies out so rapidly that binding to the RBCs will not occur to any appreciable extent. In such circumstances, changing the composition of the medium so as to retard the transport will increase the sensitivity of the method.

Plaques produced in an electric field will not be circular but will be cigar shaped. They will be similar to the patterns seen in rocket immunoelectrophoresis [16–19]. In rocket immunoelectrophoresis an electric field causes antigen from a circular well to be transported into a gel containing antibody. Antigen–antibody complexes form and subsequently a curved line of precipitate is observed. In the electrophoretic plaque technique an electric field causes antibodies emitted by a single AFC to be transported in a thin layer containing complement and RBC. Antibody binds to the RBC, lysis occurs, and subsequently a clear plaque is observed.

From the shape of the plaque the mobility of the antibodies produced by the AFC can be determined. If two plaques produced by antibodies of the same class but with different electrophoretic mobilities (the antibodies may have different net charges due to differences in their V-regions) are compared the shapes of the plaques will differ. By analyzing computer generated pictures we estimate the mobility differences of 20% or greater can easily be detected from plaque shapes. By determining the number of distinct antibody mobilities a lower bound on the number of responding clones may be obtained.

This technique seems well suited to test Cunningham's suggestion that antibody diversity can be generated after B cells have been stimulated to proliferate (Cunningham et al. [20–24]). If Cunningham is correct and single clones are studied in an electric field, one would expect to see at least some plaques from the same clone with different mobilities. One objection to Cunningham's conclusion is that AFC from the same clone which have different emission rates rather than different antibody specificities may cause the changes in plaque morphology he observes (Goldstein [25]). Such differences will not affect the determination of the mobility from plaques developed in electric fields. A second objection is that if there is a variation in the emission rate of a single AFC while the plaque is developing, its morphology in the Cunningham assay will differ from that of other cells in the same clone. To correctly determine the mobility from a plaque produced in an electric field the AFC must emit antibodies at a constant rate. However since plaques from good emitters develop rapidly in an electric field the AFC need emit at a constant rate for only a relatively short period of time. Also it is quite easy to test whether the AFC is emitting at a constant rate. After the plaque has reached its final size, reverse the field. If the AFC emission rate is constant, an identical plaque pointing in the opposite direction should develop.

Below we outline the theoretical results for the growth of plaques in the presence of an electric field. The details of the calculations are confined to the appendices.

2. The size and shape of plaques in an electric field

We now invesitgate what happens when a uniform electric field is applied to a thin layer which contains AFC, RBC, complement, and a support medium. We consider a single AFC emitting antibodies isotropically at a constant rate. The electric field will cause the antibodies to migrate with a velocity $v = \mu E$, either parallel or antiparallel to the direction of the field depending upon the sign of μ, where μ is the mobility of the antibody in the layer and E is the magnitude of the electric field. We assume that the AFC and RBC do not migrate in the electric field because of the restraint placed on them by the support medium. (The theory will not hold for liquid monolayers since the RBC and AFC, as well as the antibodies, will migrate in the electric field.)

Shortly after the AFC begins emitting antibodies a

plaque will appear and rapidly grow to its final size. To describe the plaque we use a coordinate system with the AFC at the origin and the antibody velocity in the x-direction. We use polar coordinates R and θ, where R is the distance from the AFC to the plaque boundary and θ is the angle between the x-axis and the radius vector.

The final size and shape of the plaque will depend on a number of parameters including: e, the number of binding sites per RBC (epitope density); K, the antibody–RBC affinity (for IgM, assuming single-site attachment, this is 10 times the usual antibody combining site affinity [26]; N, the number of bound antibodies per RBC at the plaque radius; h, the thickness of the layer; S, the constant antibody emission rate; D, the diffusion coefficient of the antibody in the layer; and $\gamma = v/2D$.* The plaque shape and size can be determined from the following equation derived in Appendix 2:†

$$\Omega = \exp(\gamma R \cos\theta) K_0(\gamma R), \tag{2}$$

where $K_0(\cdot)$ is a modified Bessel function of zero order [27] and

$$\Omega = 2\pi hDN/(KeS) \tag{3}$$

is a dimensionless constant. Notice that Ω depends upon the physical and geometrical properties of the system (h and D), the RBC (e, N) and properties of the AFC (K, S).

Eq. (2) depends on the two parameters, γ and Ω. Given these parameters one can use eq. (2) to obtain the plaque boundary. Conversely, given a plaque (from experiment) one can use eq. (2) to obtain γ and Ω.

2.1. Values for the plaque parameters

For IgM, $\gamma = \mu E/2D$ will range from zero to approximately 1000 cm^{-1}. Its exact value will depend on the value of the electric field used. The upper limit on γ was estimated by assuming a maximum electric field of 20 v/cm. Above 20 v/cm, heating becomes a problem in gel electrophoresis experiments [29]. (Since the times required to develop a plaque will be considerably shorter than those used in gel electrophoresis experiments higher fields might possibly be used.) The diffusion coefficient of IgM in water is 1.7×10^{-7} cm^2/s [30] while in agar gel it may be as small as 4.0×10^{-8} cm^2/s [31]. The mobility of IgM in the layer will depend on the detailed makeup of the thin layer. Marchalonis and Nossal [32] analysed antibody produced by single cells where the supporting medium used was a phoroslide TM-cellulose acetate membrane. In these experiments μ ranged from 4.8×10^{-6} $cm^2/V\,s$ to -4.0×10^{-6} $cm^2/V\,s$.‡ We expect that it is possible with other support media to obtain higher values of μ since in solution, at pH 8.6 and ionic strength 0.1, a value -2.0×10^{-5} $cm^2/V\,s$ has been obtained for the mobility of IgM [33].

The values of most of the parameters which determine Ω have been discussed in the review paper by Jerne et al. [3]. Typically $e \lesssim 6 \times 10^5$ [34–38]; for single site attachment of IgM $K \approx 10^5$ M^{-1} [39]; $S \approx 10^3$ Ab/s but values as high as 1500 Ab/s and as low as 100 Ab/s have been found in vitro† [9,40–42], and N has been estimated to be between 1 and 10 for IgM [3]. The thickness of the layer varies from the width of a monolayer to a few millimeters. For example $h = 1.2 \times 10^{-3}$ cm, in the experiments of Nossal et al. [14,15].

The value of Ω can be estimated directly from published data on the plaque size attained at $T = 1$ h in the standard thin layer plaque assay. In Appendix 1 we show [cf., eq. (1–7)]

$$2\Omega = E_1(R^2/4D^*t),$$

where D^* is the hindered diffusion coefficient discussed in section 3 and $E_1(\cdot)$ is the exponential integral of order one. (For its definition and table of values see ref. [27].) Hence given the plaque radius R, $t = 3600$ s, and the diffusion coefficient of the media, Ω can be determined.‡ In fig. 1 we plot Ω versus R for

* The parameter γ is related to the dimensionless Peclet number, P. If L is a characteristic length, on the order of a typical plaque radius, then $P = vL/D = 2\gamma L$ [28].

† Eq. (2) is an exact result. No assumptions are made about local equilibrium or the type of binding. Of course, since it is a steady state result, local equilibrium is certainly obtained.

‡ In the primary response, migration distances d ranged from +6 mm to −5 mm, $E = 35$ V/cm and $t = 1$ h. μ was calculated from the formula $\mu = d/tE$.

† Values as high as 2×10^4 Ab/s have been found in vivo [43].

‡ This overestimates t since the cell may not have emitted antibodies for the full hour. Consequently Ω is also overestimated.

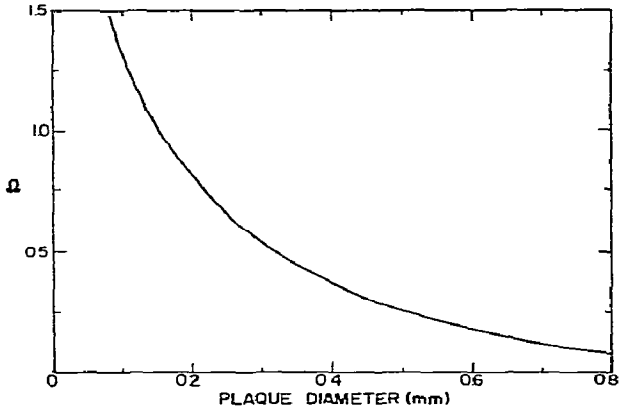

Fig. 1. Conversion of plaque diameter to Ω values for $D^* = 8 \times 10^{-8}\,cm^2/s$ and $t = 3600$ s.

$D^* = 8 \times 10^{-8}\,cm^2/s$. Using this procedure various experiments have been analyzed. The ranges of Ω found are shown in table 1. In the experiments of Merchant and Peterson [4] the distribution of plaque diameters was given for both RBC antigen and an arsenate hapten. For both experiments over 90% of the plaques had Ω values less than one.

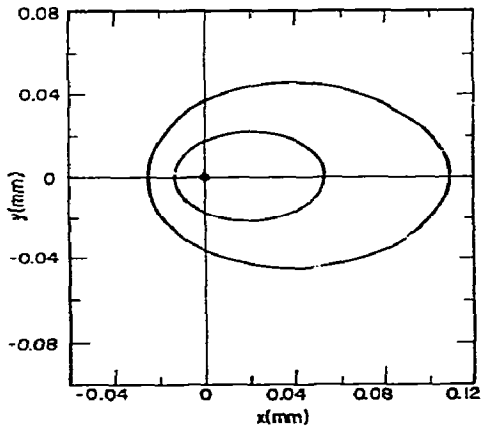

Fig. 2. The effect of electric field on plaque size. For both plaques Ω = 1.0. The outer plaque corresponds to $\gamma = 125\ cm^{-1}$ while the inner plaque corresponds to $\gamma = 250\ cm^{-1}$. Since $\gamma = \mu E/2D$ doubling E would change γ from 125 to 250 cm^{-1}. Typical value of μ, D and E that give these values of γ are $\mu = 4 \times 10^{-6}\ cm^2/V\,s$, $D = 8 \times 10^{-8}\,cm^2/s$ and $E = 5$ V/cm and 10 V/cm.

Table 1
Experimental range of Ω for direct plaques [a]

Range of Ω	Mean value of Ω	Ref.
1.4–0.10	0.54	[4]
2.8–0.77	0.95	[15]
0.8–0.18	–	[53]
1.1–0.13	–	[20]

a) All the cited experiments except those of Cunningham and Forsham [20] and Merchant and Peterson [4], were done in the presence of a support material. For these experiments a value of $D^* = 8 \times 10^{-8}\ cm^2/s$ was used to find Ω. These experiments were performed in a liquid monolay for which $D^* \approx 1.7 \times 10^{-7}\ cm^2/s$. The illustrated value of Ω has been adjusted so as to correspond to $D^* = 8 \times 10^{-8}\ cm^2/s$.

2.2. Plaque shapes

For given values of γ and Ω eq. (2) can be solved numerically to give the coordinates of the plaque boundary. Although there are many ways to do this, a straightforward method is to choose a θ value and then evaluate the product $\exp(\omega \cos\theta) K_0(\omega)$ for various ω values. (This can be done with a table of $K_0(\omega)$ values [27] and a pocket calculator.) This is continued until the ω is found for which $\Omega = \exp(\omega \cos\theta) K_0(\omega)$. For this value of ω, $R = \omega/\gamma$. This can be repeated for as many values of θ as is desired. For greater speed and accuracy a digital computer and more sophisticated algorithms, such as Newton's method, can be utilized.

In fig. 2 the effect of the electric field on the plaque size is shown. The smaller plaque was produced in a field twice as large as the field producing the larger plaque. Increasing E always decreases the final plaque size. We will see in the next section that increasing E also decreases the time needed to obtain the final plaque size. Thus one wants to use some intermediate value of E, large enough so the plaques develop rapidly, but small enough so the plaques are of reasonable size.

The fact that increasing E decreases the plaque size can be seen directly from eq. (2). The left side is independent of E. For a given value of θ the right side of eq. (2) is only a function of γR. This means that changing γ scales the size of the plaque. Since γ is proportional to E, it follows that for any value of θ, R is proportional to $1/E$. Heuristically one can understand this behavior as follows. At steady state the rate at which antibodies are

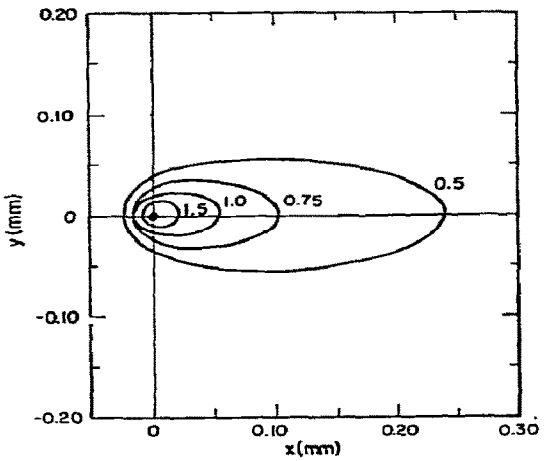

Fig. 3. The effects of varying Ω for constant γ. For all curves $\gamma = 250\ cm^{-1}$; $\Omega = 0.5, 0.75, 1.0$, and 1.5.

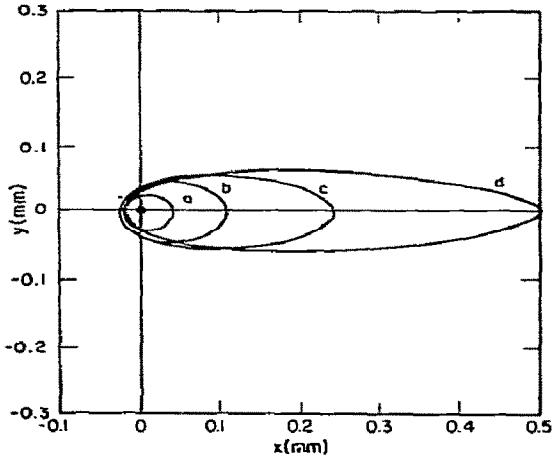

Fig. 4. The effect of variations in the diffusion coefficient on plaque size. All parameters except D were held constant, i.e., $\Omega/D = 1.25 \times 10\ s/cm^2$ and $\gamma D = 10^{-5}$ cm/s. For curves a, b, c and d, $D = 1.6 \times 10^{-7}$, 8×10^{-8}, 4×10^{-8} and 2×10^{-8} cm/s respectively. Notice curve b which corresponds to $\Omega = 1.0$, $\gamma = 1.25\ cm^{-1}$ and $D = 8 \times 10^{-8}\ cm^2/s$ is the same as the outer curve in fig. 2.

transported from the AFC to some volume element centered at position (R, θ) is counterbalanced by the rate at which they are transported out of the volume element. Increasing E, increases the transport rate and hence more antibodies will be lost by transport out of the volume element. This lowers the antibody concentration at (R, θ) and one must move closer to the AFC to find sufficient antibody to lyse a RBC. Thus the plaque size decreases. Because the transport rates have increased these smaller plaques will form more rapidly.

Notice even when $E \neq 0$, γ will be zero if the secreted antibody is uncharged (i.e., $\mu = 0$). Hence spherical plaques which grow unbounded can be obtained in the presence of an electrical field.

In fig. 3 γ is held constant and Ω is varied. As Ω increases, the size of the plaque decreases (this follows from the fact that as x is decreased, $\exp(x) K_0(x)$ increases). Thus, increasing S, K or e, or decreasing h or N will increase the plaque size. For example, if the inner most plaque corresponded to $S = 500$ Ab/s then for the outer most plaque $S = 1500$ Ab/s.

In fig. 4 the diffusion coefficient is varied while all other parameters are held constant. (Experimentally D can be changed by changing the composition of the layer. For example, one can change the agar concentration or the RBC concentration.) When no field is present the plaque radius does not reach a steady state. However, at a fixed time, increasing D will increase the plaque diameter for small values of D and decrease the plaque diameter after some critical value depending upon K, e, S, h and N, is reached [13]. This decrease in the plaque radius is due to the lowering of the antibody concentrations near the AFC by its rapid diffusion away. When there is any electric field present and $\mu \neq 0$ a plaque will reach a steady state size. How the steady state value of R changes with D depends on the values of θ, γ, and Ω. As can be seen from fig. 4, for reasonable values of the parameters increasing D decreases the plaque radius in the forward ($\theta = 0$) direction.

2.3. Analyzing plaque data

Given a plaque which has developed in an electric field one should be able to determine γ and Ω.

For an experiment done in an electrical field with magnitude E, $\gamma = \mu E/2D$. Hence, from γ the ratio μ/D can be found. A variation in the V-region of an IgM antibody will not effect D and hence changes in antibody charge can be ascertained from studies of γ. For most immunological applications D need not be determined. To obtain the absolute value of μ a separate determination of D would need to be done.

One way to determine γ is from the values of R and

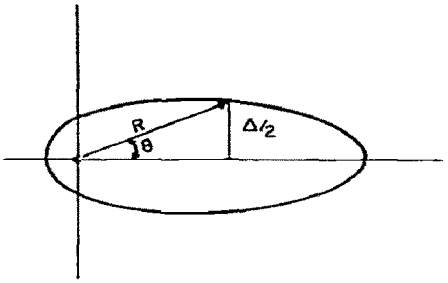

Fig. 5. Typical plaque with R, θ and the plaque width Δ illustrated.

θ at which the plaque width, Δ, is a maximum. We call these values R^* and θ^* (see fig. 5). These values satisfy the following equation (see Appendix 3):

$$K_1(\gamma R^*)/K_0(\gamma R^*) = 1/\cos\theta^*. \tag{4}$$

where $K_0(\cdot)$ and $K_1(\cdot)$ are modified Bessel functions [27]. This is a transcendental equation for γ. One can calculate $K_1(x)/K_0(x)$ for any x from the tables, or from the equations (9.8.5–9.8.8) on p. 375 of ref. [27].

We expect that in most cases $\gamma R^* \gg 1$. When this condition holds, eq. (4) can be reduced to the following equation:

$$\gamma = \frac{1}{2R^*\,[1-(3-2/\cos\theta^*)^{1/2}]} \tag{5}$$

When $\gamma R^* \gg 1$ a second method can be used to analyze plaque shapes. There will be a wide range of R values for which $\gamma R \gg 1$. For these values the following equation holds (see Appendix 3):

$$-\ln R = 2\gamma R(1-\cos\theta) + 2\ln\Theta, \tag{6}$$

where $\Theta = (2\gamma/\pi)^{1/2}\,\Omega$.

If one plots $-\ln R$ against $R(1-\cos\theta)$ a straight line with a slope of 2γ and an intercept of $2\ln\Theta$ will be obtained. From the slope and intercept γ and Ω can be determined.

3. The time development of plaques in an electric field

To see how long it takes for plaques in an electric field to reach their final size, we need expressions which describe the position of the plaque boundary as a function of time. We again consider an AFC in a thin layer which emits antibodies at a constant rate. The AFC is placed in the layer at time $T = 0$ and begins emitting antibodies at time $T = T_0$. We set $t = T - T_0$, where t is the total emission time of the AFC and T is the total time it has been in the layer.

The equation from which plaque shape and size can be determined for any time, and which reduces to eq. (2) when t goes to infinity, is (all equations in this section are derived in Appendix 4):*

$$\Omega = \tfrac{1}{2}\exp(\gamma R\cos\theta)\int_{\beta}^{\infty}\frac{\exp[-u-(\gamma R)^2/4u]}{u}\,du, \tag{7}$$

where $\beta = R^2/4D^*t$ and D^* is the hindered diffusion coefficient.†

In figs. 6 and 7 the time development of two plaques are shown with the electric field both on and off. In these cases the plaques in the presence of the field quickly come to their asymptotic limit. In order to compare the $E = 0$ and $E \neq 0$ cases, in fig. 8 we have plotted the plaque area versus time. Notice that the plaques developed by the standard assay reach a comparable size in the same time period, so no sensitivity is gained by using the electric field. At longer times the plaques in the absence of a field continue to grow and hence eventually become larger than their cigar-shaped counterparts.

3.1. Approximate expressions for short and long times

From eq. (7) approximate expressions which hold at short and long times can be derived. These expressions depend on the dimensionless parameter α where

$$\alpha = \gamma^2 D^* t. \tag{8}$$

* Eq. (7) is an approximate result. The key assumption made in obtaining eq. (7) is that there is local equilibrium between the free and bound antibody concentrations.

† Because of the binding of the antibodies to RBC, free antibody appears to diffuse with a diffusion coefficient D^* which is smaller than the true diffusion coefficient D. $D^* = D/(1 + K\rho_0)$, where ρ_0 is the binding site concentration, i.e., $\rho_0 = e\rho_{RBC}$, where e is the number of sites per RBC and ρ_{RBC} is the RBC concentration in the layer [44]. In plaque experiments where IgM binds only through single site attachment the difference between D^* and D is negligible (for $K = 10^5\ M^{-1}$, $e = 10^5$ and $\rho_{RBC} = 2\times10^8$, a typical RBC concentration in plaque experiments, $K\rho_0 = 3.3\times10^{-3}$ and hence $D^* = 0.9967\,D$).

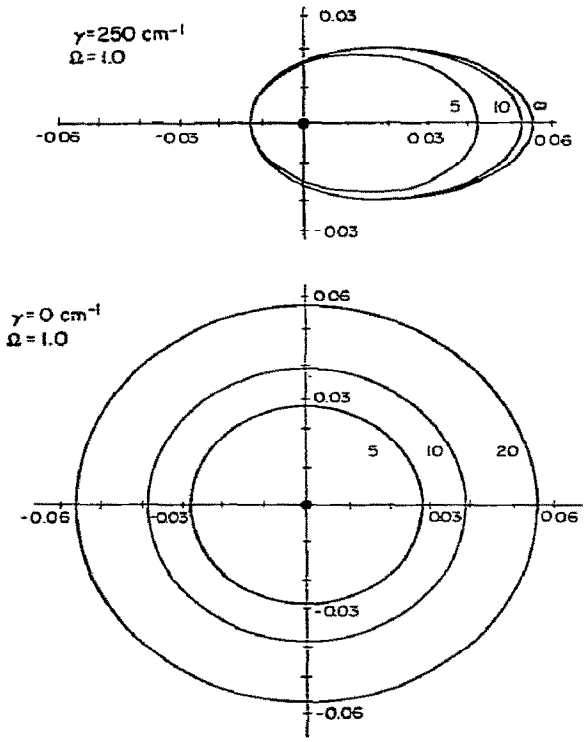

Fig. 6. Temporal development of a plaque. The curves shown are for $\Omega = 1.0$. (a) Field on, $\gamma = 250\ cm^{-1}$. (b) Field off, $\gamma = 0\ cm^{-1}$. Distances along the x and y axes are measured in mm. Times are measured in minutes and (∞) labels the steady state plaque.

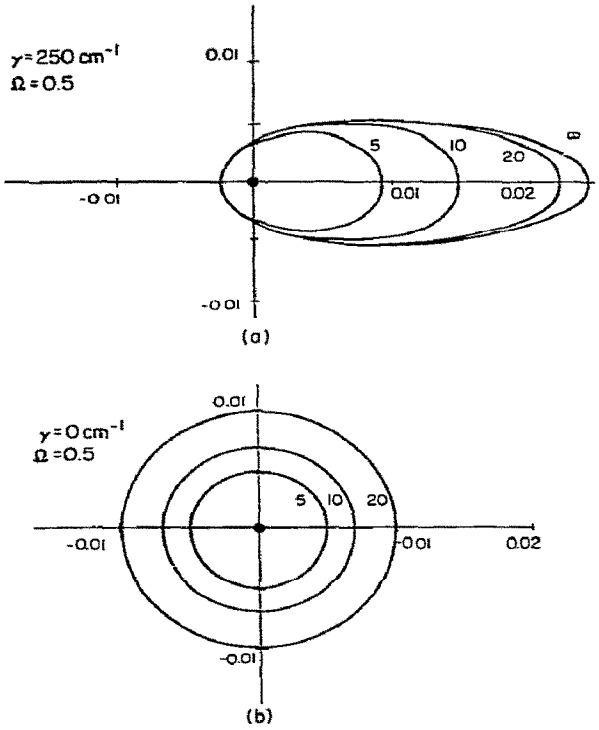

Fig. 7. Temporal development of a plaque formed by a good emitter, $\Omega = 0.5$. (a) Field on, $\gamma = 250\ cm^{-1}$. (b) Field off, $\gamma = 0\ cm^{-1}$. Distances along the x and y axes are measured in mm. Times are measured in minutes and (∞) labels the steady state plaque.

To see why this parameter is important we introduce two characteristic lengths, the characteristic transport length $L_E = vt$, and the characteristic diffusion length $L_D = (4D^*t)^{1/2}$. In terms of these lengths $\alpha = (L_E/L_0)^2 (D^*/D)^2$. Since, in plaque experiments $D^* \approx D$, when $\alpha \gg 1$ transport dominates diffusion (for large enough times this will always be true), while when $\alpha \ll 1$ diffusion dominates transport (for small enough times this will always be the case since the concentration gradients will be very large).

For $\alpha \ll 1$ eq. (7) becomes:

$$2\Omega = \exp(\gamma R \cos\theta)\left(E_1(\beta) - \alpha E_2(\beta) + \frac{1}{2!}\alpha^2 E_3(\beta) \ldots\right), \tag{9}$$

where $E_n(\cdot)$ is the exponential integral of order n (for its definition and a table of its values see ref. [27], ch. 5). When γ is set equal to zero eq. (9) reduces to the equation for a plaque in the absence of a field (see Appendix 1, eq. 1–7).

For $\alpha \gg 1$ eq. (7) becomes:

$$\Omega = \exp(\gamma R \cos\theta) \times \left\{K_0(\gamma R) - \frac{1}{2}\left(E_1(\alpha) - \beta E_2(\alpha) + \frac{\beta^2}{2!} E_3(\alpha) \ldots\right)\right\}. \tag{10}$$

As t goes to infinity, α goes to infinity and all the $E_n(\alpha)$ go to zero. Thus, for long times eq. (10) reduces to eq. (2), the steady state result.

In Appendix 5 we show how eq. (10) can be used to estimate the time, t_{ss}, it takes for a plaque to reach its

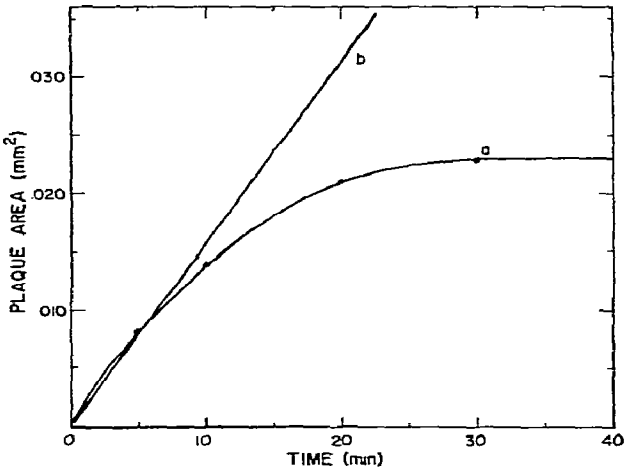

Fig. 8. Comparison of the time development of plaque areas for a good emitter with and without an electric field, $\Omega = 0.5$. (a) $\gamma = 250\ \mathrm{cm}^{-1}$, (b) $\gamma = 0$.

final size in an electric field. Simply stated the plaque will reach a given radius R when $\frac{1}{2} E_1(\alpha) \gg K_0(\gamma R)$. Typically this will occur for α greater than 1 but less than 10, i.e., $t_{ss} \approx m/\gamma D^*$, where m is between 1 and 10.

The mathematical approach used in deriving eq. (7) is rather general and is applicable to other models of plaque formation. If instead of assuming that antibody molecules reversibly bind to RBC and quickly establish an equilibrium between free and bound forms, we assume that binding is irreversible with forward rate constant k_1, then we find

$$\Omega^* = \exp(\gamma R \cos\theta) \int_{\beta'}^{\infty} \frac{\exp[-u - (\gamma^* R)^2/4u]}{u}\, du,$$

where $\gamma^* = (\gamma^2 + k_1 \rho_0/D)^{1/2}$, $\Omega^* = 2\pi h D N/k_1 e S t$, and $\beta' = R^2/4Dt$. Since a bound antibody is sure to dissociate if one waits long enough, the irreversible binding approximation can only be valid for finite times. We feel that the assumption of reversible binding of IgM is more appropriate and consequently have not pursued other binding assumptions. For a general discussion of irreversible binding see refs. [12,45,46].

4. Conclusion

The theoretical results presented in this paper suggest that there are advantages in performing the direct hemolytic plaque technique in an electric field. Our work indicates that in the presence of an electric field a plaque will reach a steady state. The plaque will be cigar shaped unless, of course, the secreted antibodies are uncharged. We have shown how such a plaque can be analyzed to determine the mobility of the secreted antibodies. The larger the electric field used, the faster the plaque will develop. However, increasing the electric field decreases the final plaque size. For any particular experimental system, one must find the appropriate electric field and media composition to work at in order that the plaques develop rapidly and are of reasonable size.

We feel that the theoretical studies presented in this paper justify an effort to develop the electrophoretic hemolytic plaque technique.

Acknowledgement

We thank George Bell for his thoughtful comments and criticisms. We also acknowledge Mrs. Mary Plehn's help in the preparation of this manuscript.

Appendix 1. Mathematical theory of IgM plaque growth in two dimensions

In this appendix we outline the mathematicl theory of the growth of direct placques in thin layers which contain RBCs and complement. In particular, we consider an AFC in a thin layer of thickness h. Assume the AFC emits IgM antibodies at a constant rate S, beginning at time t_0 and that these antibodies diffuse in the layer with a constant diffusion coefficient D. Also, assume that in the layer the IgM undergoes reversible binding to various sites on the RBC surfaces.

The mathematical model we shall outline assumes that the free antibody concentration $c(x, y, z, t)$ is uniform in the z-direction and hence that diffusion only occurs in two dimensions. (For monolayers this will certainly be a good approximation, but for much thicker layers vertical concentration gradients could develop and diffusion perpendicular as well as parallel to the layer

will be important. For such layers the detailed effects of the finite width of the layer must be considered.)

Since we assume that diffusion is confined to a plane, we shall model the AFC as an isotropic cylindrical emitter of antibodies. Taking the emission to be isotropic assures that when there is no field present the plaques are circular.

To model the binding of IgM to an RBC we use a greatly simplified description and introduce only two rate constants, k_1, an overall forward rate constant and k_2, an overall reverse rate constant. In terms of these rate constants, the free antibody concentration, c, and the bound site concentration, ρ, obey the following equations [the AFC is taken to be at the origin ($r = 0$) of our coordinate system]

$$\frac{\partial c}{\partial t} = D\nabla^2 c - \frac{\partial \rho}{\partial t} + \frac{S(t)}{h}\delta(r), \tag{1–1}$$

$$\partial\rho/\partial t = k_1 c(\rho_0 - \rho) - k_2\rho, \tag{1–2}$$

where ρ_0 is the initial concentration of free binding sites, i.e., $\rho_0 = e\rho_{RBC}$, where e is the number of binding sites per RBC (the epitope density), and ρ_{RBC} is the RBC concentration in the layer. $\delta(r)$ is the two-dimensional Dirac delta function [$\delta(r) = \delta(x)\,\delta(y)$]. The integral of $\delta(r)$ over any area which includes the origin equals one.

Eq. (1–1) describes how the free antibody concentration changes with time at any point in the layer: by diffusion; by loss or gain of antibodies through binding to, or release from, RBC surfaces; and, at the origin, by the production of antibodies at a rate $S(t)$.

The rate of change in the bound site concentration is described by eq. (1–2). The rate of binding of antibodies to RBCs is assumed to be proportional to the product of the free antibody concentration and the free site concentration. The rate of release of bound antibodies from the RBC surface is assumed to be simply proportional to the concentration of bound sites.

To solve eqs. (1–1) and (1–2) we make two additional assumptions. First we assume that the fraction of sites bound on any single RBC is small and hence $\rho_0 - \rho \approx \rho_0$. The justification for this is that the free antibody concentrations which arise in a layer from the emission of antibodies by an AFC, at least for times less than many hours, are not high enough to cause a large fraction of the sites to be bound. (A possible exception is the few RBC which may be in the immediate vicinity of the AFC.) With this assumption eq. (1–2) becomes

$$\partial\rho/\partial t = k_1 c\rho_0 - k_2\rho. \tag{1–3}$$

The second assumption is that there is local equilibrium between the free and bound antibody concentrations. Since the bound antibody concentration is directly proportional to the bound site concentration, the local equilibrium assumption, can be written as follows:

$$\rho = K\rho_0 c, \tag{1–4}$$

where $K = k_1/k_2$. The justification for this assumption is that with it, the theory predicts the observed time development for direct plaques. Although at first sight it may seem surprising that for IgM, a molecule capable of forming very strong multisite attachments [39], local equilibrium occurs with RBC antigens, we are led to this conclusion from the results of time studies on the growth of direct plaques [8,14,15]. For a detailed discussion of when it is appropriate to approximate eq. (1–3) by eq. (1–4), see ref. [44].

If we differentiate eq. (1–4) with respect to time and substitute into eq. (1–1), the equation for c becomes

$$-\frac{S(t)}{hD}\delta(r) = \nabla^2 c - \frac{1}{D^*}\frac{\partial c}{\partial t}, \tag{1–5}$$

where $D^* = D/(1 + K\rho_0)$ and $S(t) = \begin{cases} 0 & t < 0 \\ S & t \geqslant 0 \end{cases}$. This is just the diffusion or heat equation for a point source in two dimension, the solution of which is (see, for example, eq. (5) on p. 261 of ref. [47]:

$$c(r, t) = (S/4\pi Dh)\,E_1(r^2/4D^*t), \tag{1–6}$$

where r is the radial distance from the AFC and $E_1(\cdot)$ is the exponential integral of order 1.

To obtain an equation for the plaque radius as a function of time we assume that at the plaque radius there are N antibodies bound per RBC (Jerne [3] has estimated N to be between 1 and 10 for IgM). Thus, at the plaque radius, $\rho = N\rho_{RBC}$ and from eqs. (1–4) and (1–6) if follows that

$$4\pi DhN/KeS = E_1(R^2/4D^*t), \tag{1–7}$$

where R is the plaque radius.

Since the left side of eq. (1–7) is a constant for any particular AFC, the right side must also be constant. The

only way this can be is if the argument of E_1 is a constant, i.e.,

$$R^2/4D^*t = \text{const.}, \tag{1–8}$$

from which eq. (1) in the text follows.

Experimentally it has been found that eq. (1–8) holds for direct plaques and RBC antigens. If haptenated RBC are used, eq. (1–8) will still hold if the hapten density is such that only single site attachment can occur.[‡] [For single site attachment IgM will rapidly dissociate [39] and after very short times local equilibrium will obtain.) To insure that single site attachment is the predominant type of binding, the average spacing between haptens on the RBC surface should be larger than the largest distance between the antigen binding sites on IgM, approximately 350 Å. For a RBC with a surface area of $1.4 \times 10^{-6}\text{cm}^2$ [49,50] $e < 1.1 \times 10^5$ will satisfy this condition.

Appendix 2. Steady state solution to the plaque equations in the presence of an electric field

Once again consider an AFC, placed at $r = 0$ in a layer of thickness h, which for $T \geqslant T_0$ emits S antibodies per second. Now, however, we shall not make either of the assumptions of Appendix 1 (i.e., low epitope density and local equilibrium). Further assume that there is an electric field in the x-direction. The antibody flux, anywhere in the layer, except at $r = 0$, is

$$J = -D\nabla c + vc\vec{i}, \tag{2–1}$$

where $\vec{i}$ is a unit vector in the x-direction, c is the free antibody concentration, ∇c is the gradient of the free antibody concentration, D is the diffusion coefficient of the antibody in the gel and $v = \mu E$ (μ is the antibody mobility and E is the magnitude of the electric field). The component of J in any direction is the number of moles of antibody passing a unit area, perpendicular to the direction, per unit time.

In the steady state the free and bound antibody concentrations are constant. Therefore, for any closed volume V of gel with thickness h, the net number of antibodies crossing the boundary of V per unit time equals the number produced per unit time within V, i.e.,

$$\nabla \cdot J = S\,\delta(r)/h. \tag{2–2}$$

If we combine eqs. (2–1) and (2–2) assuming D is constant we obtain the equation

$$-(S/h)\,\delta(r) = D\nabla^2 c - v\,\partial c/\partial x. \tag{2–3}$$

Making the substitution

$$c = \exp(\gamma x)\,g, \tag{2–4}$$

where $\gamma = v/2D$, eq. (2–3) becomes

$$-(S/Dh)\exp(-\gamma x)\,\delta(r) = (\nabla^2 - \gamma^2)g. \tag{2–5}$$

The solution of eq. (2–5) in 2 dimensions which goes to zero as r approaches infinity is

$$g = (S/2\pi hD)\,K_0(\gamma r), \tag{2–6}$$

where $K_0(\cdot)$ is a modified Bessel function [27].

This solution was obtained in the following way. The Fourier transform of eq. (2–5) is

$$\bar{g}(k) = \frac{S}{(2\pi)^2 hD}\,\frac{1}{k^2 + \gamma^2}, \tag{2–7}$$

where $\bar{g}(k)$ is the transform of $g(r)$, i.e.,

$$g(r) = \int_{-\infty}^{\infty} \exp(i\vec{k}\cdot\vec{r})\,\bar{g}(k)\,\mathrm{d}^2k. \tag{2–8}$$

If we substitute eq. (2–7) into (2–8) and perform the angular integration,

$$g(r) = \frac{S}{2\pi hD}\int_0^{\infty} \frac{k\,\mathrm{d}k\,J_0(kr)}{k^2 + \gamma^2}. \tag{2–9}$$

This integral is known (see eq. (4) on p. 678 in ref. [51]), the result being eq. (2–6).

From eqs. (2–4) and (2–6) we have that the free antibody concentration is

$$c(r,\theta) = (S/2\pi hD)\exp(\gamma r\cos\theta)\,K_0(\gamma r), \tag{2–10}$$

where $x = r\cos\theta$.

In the steady state $\partial\rho/\partial t = 0$ and hence from eq. (1–2) the bound antibody concentration $\rho = Kc\rho_0/(1 + Kc)$.

[‡] Even if some multisite attachment occurs due to the diffusion of the surface molecules on the RBC membrane, local equilibrium will still be obtained as long as the single site association–dissociation rates are fast compared to the rate of multisite attachment [26]. Since capping is not usually observed on RBC [48] the mobility of surface RBC components is probably restricted.

At the plaque radius $1 \gg Kc$, so that,

$$\rho(R, \theta) = Ke\rho_{RBC}\, c(R, \theta). \quad (2-11)$$

Setting $\rho(R, \theta) = N\rho_{RBC}$ at the plaque radius, where N is the number of antibodies bound per RBC, we find

$$N = (KeS/2\pi hD) \exp(\gamma R \cos\theta) K_0(\gamma R) \quad (2-12)$$

from which eq. (2) follows.

Appendix 3. Determining AFC parameters from the plaque shape

Maximum plaque width – In this appendix we find an expression for the maximum width, Δ^*, of a plaque formed in an electric field. From fig. 5 it can be seen that the plaque width, Δ, at position (R, θ) on the plaque boundary is given by

$$\Delta = 2R \sin\theta. \quad (3-1)$$

To find the values of R and θ at the maximum width, we calculate $d\Delta/d\theta$ and set it equal to zero.

$$\frac{d\Delta}{d\theta} = \frac{\partial\Delta}{\partial\theta} + \frac{\partial\Delta}{\partial R}\frac{\partial R}{\partial\theta}.$$

Since $\Delta = 2R \sin\theta$,

$$d\Delta/d\theta = 2R\cos\theta + 2\sin\theta\, \partial R/\partial\theta. \quad (3-2)$$

At $\Delta = \Delta^*$, $d\Delta/d\theta = 0$ and eq. (3–2) becomes

$$\partial R/\partial\theta = -R^* \cot\theta^*. \quad (3-3)$$

If we now differentiate eq. (2), the equation for the plaque, and solve for $\partial R/\partial\theta$ we obtain

$$\partial R/\partial\theta = R\sin\theta/[\cos\theta - K_1(\gamma R)/K_0(\gamma R)]. \quad (3-4)$$

Setting eq. (3–3) equal to (3–4), cross multiplying and using the identity $\cos^2\theta + \sin^2\theta = 1$, eq. (4) follows, i.e.,

$$K_1(\gamma R^*)/K_0(\gamma R^*) = 1/\cos\theta^*. \quad (3-5)$$

When $\gamma R^* \gg 1$ we can use the asymptotic expansions for the modified Bessel functions (see eq. 9.7.2 on p. 378 of ref. [27]) to approximate the left hand side of eq. (3–5). To second order in $1/\gamma R^*$, eq. (3–5) becomes

$$1 + 1/2\gamma R^* - 1/8(\gamma R^*)^2 = 1/\cos\theta^*. \quad (3-6)$$

This is a quadratic equation in $1/\gamma R^*$, the solution of which is

$$1/2\gamma R^* = 1 - (3 - 2/\cos\theta^*)^{1/2}, \quad (3-7)$$

and hence

$$\gamma = \frac{1}{2R^*[1 - (3 - 2/\cos\theta^*)^{1/2}]}. \quad (3-8)$$

Approximate equation for the plaque boundary – When $\gamma R \gg 1$,

$$K_0(\gamma r) \approx (\pi/2\gamma R)^{1/2} \exp(-\gamma R). \quad (3-9)$$

(see eq. 9.7.2 on p. 378 of ref. [27].)

If we substitute eq. (3–9) into eq. (2) we obtain,

$$(2\gamma R/\pi)^{1/2}\Omega = \exp[\gamma R(\cos\theta - 1)]. \quad (3-10)$$

Taking the natural logorithm of eq. (3–10)

$$-\ln R = 2\gamma R(1 - \cos\theta) + 2\ln\Theta, \quad (3-11)$$

where $\Theta = (2\gamma/\pi)^{1/2}\Omega$.

Appendix 4. Time dependent plaque growth

The set of equations which describe the growth of direct plaques in thin layers in the presence of a uniform electric field E are the same as those in Appendix 1 (the $E = 0$ case) with one difference. With an electric field present the rate of change of the free antibody concentration is

$$\frac{\partial c}{\partial t} = D\nabla^2 c - v\frac{\partial c}{\partial x} - \frac{\partial\rho}{\partial t} + \frac{S}{h}\delta(r), \quad (4-1)$$

where the electric field has been taken to be in the x direction. The term $v\,\partial c/\partial x$ follows from the fact that the flux due to the electric field is $vc\hat{i}$, where $\hat{i}$ is a unit vector in the x-direction. Here $t = T - T_0$, the duration time.

The equation for the bound site concentration remains unchanged,

$$\partial\rho/\partial t = k_1 c(\rho_0 - \rho) - k_2\rho. \quad (4-2)$$

We now make the same two assumptions we made in Appendix 1. We assume the fraction of sites that are bound on any single RBC is small, and that there is local equilibrium between the free and bound antibody concentrations. With these assumptions eq. (4–1) becomes

$$\frac{1}{D^*}\frac{\partial c}{\partial t} = \nabla^2 c - 2\gamma\frac{\partial c}{\partial x} + \frac{S}{Dh}\delta(r), \qquad (4\text{–}3a)$$

where $D^* = D/(1 + K\rho_0)$ and $\gamma = v/2D$. For all points in the layer except at $r = 0$,

$$c(r, t = 0) = 0. \qquad (4\text{–}3b)$$

Taking the Laplace transform of eq. (4–3), and indicating the transforms of $c(r, t)$ and $S(t)$ by $\bar{c}(r, p)$ and $\bar{S}(p)$, respectively, we obtain

$$-(\bar{S}/hD)\delta(r) = \nabla^2\bar{c} - 2\gamma(\partial\bar{c}/\partial x) - q^2\bar{c}, \qquad (4\text{–}4)$$

where $q^2 = p/D^*$.

If we let

$$\bar{c} = \bar{g}\exp(\gamma x), \qquad (4\text{–}5)$$

eq. (4–5) becomes

$$-(\bar{S}/hD)\delta(r)\exp(-\gamma x) = (\nabla^2 - q'^2)\bar{g}(r, p), \qquad (4\text{–}6)$$

where $q'^2 = q^2 + \gamma^2$. (For irreversible binding, i.e., $k_2 = 0$, and $\rho_0 - \rho \approx \rho_0$, eq. (4–2) becomes $\partial\rho/\partial t = k_1\rho_0 c$. It is easy to see that eq. (4–6) would not change, but q'^2 would equal $p/D + \gamma^2 + k_1\rho_0/D$.)

An equation of this form was solved in Appendix 2. From eq. (2–6) it follows that

$$\bar{g}(r, p) = (\bar{S}/2\pi hD)K_0(q'r). \qquad (4\text{–}7)$$

Assuming the emission rate is constant, $\bar{S} = S/p$, and

$$\bar{g}(r, p) = (S/2\pi hDp)K_0(q'r). \qquad (4\text{–}8)$$

Transforming back we obtain

$$g(r, t) = (S/4\pi hD)\int_0^t \frac{\exp(-\gamma^2 D^* t' - r^2/4D^* t')}{t'}\,dt' \qquad (4\text{–}9)$$

(see ref. [52], eq. 1 on p. 304 and eqs. 3 and 13 on pp. 169 and 170).

If we let $\beta = r^2/4D^*t$ and $u = r^2/4D^*t'$, eq. (4–9) becomes

$$g(r, t) = (S/4\pi hD)\int_\beta^\infty \frac{\exp(-u - (\gamma r)^2/4u)}{u}\,du. \qquad (4\text{–}10)$$

From eqs. (4–5) and (4–10) the expression for c given in section 3, eq. (7), is obtained:

$$c(r, t) = \frac{S}{4\pi Dh}\exp(\gamma r\cos\theta) \times \int_\beta^\infty \frac{\exp[-u - (\gamma r)^2/4u]}{u}\,du. \qquad (4\text{–}11)$$

Observing that

$$(\gamma r)^2/4\beta = \gamma^2 D^* t = \alpha, \qquad (4\text{–}12)$$

we see that for $\alpha \ll 1$

$$c(r, t) = \frac{S}{4\pi Dh}\exp(\gamma r\cos\theta) \times \int_\beta^\infty \frac{\exp(-u)}{u}\left[1 - \left(\frac{\gamma r}{2}\right)^2\frac{1}{u} + \frac{1}{2!}\left(\frac{\gamma r}{2}\right)^4\frac{1}{u^2} + \ldots\right]du. \qquad (4\text{–}13)$$

Since

$$E_n(\beta) = \int_1^\infty t^{-n}\exp(-\beta t)\,dt = \beta^{n-1}\int_\beta^\infty u^{-n}\exp(-u)\,du, \qquad (4\text{–}14)$$

eq. (4–13) can be rewritten as

$$c(r, t) = \frac{S}{4\pi Dh}\exp(\gamma r\cos\theta)\left[E_1(\beta) - \alpha E_2(\beta) + \frac{1}{2!}\alpha^3 E_3(\beta)\ldots\right]. \qquad (4\text{–}15)$$

This is eq. (9) in the text.

To obtain the long-time limit, $\alpha \gg 1$, we rewrite eq. (4–11) as

$$c(r, t) = \frac{S}{4\pi Dh}\exp(\gamma r\cos\theta) \times \int_0^t (t')^{-1}\exp(-r^2/4D^* t')\exp(-\gamma^2 D^* t')\,dt'. \qquad (4\text{–}16)$$

Writing the integral from zero to t, $I(0, t)$, as $I(0, \infty) - I(t, \infty)$ and using eq. 9 on p. 340 of ref. [51] we obtain:

$$c(r, t) = \frac{S}{2\pi Dh}\exp(\gamma r\cos\theta)\left[K_0(\gamma r) - \tfrac{1}{2}\int_t^\infty (t')^{-1}\exp(-\gamma^2 D^* t')\exp(-r^2/4D^* t')dt'\right]. \qquad (4\text{–}17)$$

For large t, we can expand $\exp(-r^2/4D^*t')$. Changing integration variable to $u = t'/t$ gives

$$c(r,t) = \frac{S}{2\pi Dh}\exp(\gamma r\cos\theta)\left[K_0(\gamma r) - \tfrac{1}{2}\int_1^\infty \exp(-\alpha u)\frac{du}{u}\left(1 - \frac{\beta}{u} + \frac{1}{2!}\frac{\beta^2}{u^2}\cdots\right)\right]$$

$$= \frac{S}{2\pi Dh}\exp(\gamma r\cos\theta)\left[K_0(\gamma r) - \tfrac{1}{2}\left(E_1(\alpha) - \beta E_2(\alpha) + \frac{\beta^2}{2!}E_3(\alpha)\cdots\right)\right], \qquad (4\text{–}18)$$

which is eq. (10).

Appendix 5. Estimation of the time it takes a plaque to reach its final size in an electric field

Comparing eqs. (10) and (2) we see that when

$$\tfrac{1}{2}\left(E_1(\alpha) - \beta E_2(\alpha) + \frac{\beta^2}{2!}E_3(\alpha)\cdots\right) \ll K_0(\gamma R), \qquad (5\text{–}1)$$

the plaque will approximate its final size. Since β is typically less than 1 and $E_{n+1} < E_n$, we can approximate the left hand side of eq. (5–1) by the first term $\frac{1}{2}E_1(\alpha)$. Now say we want to estimate the time it took the inner plaque ($\gamma = 25$, $\Omega = 1$) in fig. 2 to reach its steady state size. In the $\theta = 0$ direction, $R \approx 0.054$ mm and hence $\gamma R = 1.35$ and $K_0(\gamma R) \approx 0.37$. If we require $\frac{1}{2}E_1(\alpha)$ to equal $0.01\,K_0(\gamma R)$, then we find $\alpha \approx 3.5$. This value of α corresponds to $t_{ss} = 11.7$ min. In fig. 6a we show the computed time development of the plaque. The plaque at t_{ss} would be indistinguishable from the steady state plaque in an experimental situation.

For directions other than $\theta = 0$, R is smaller at the plaque boundary and hence $K_0(\gamma R)$, which decreases monotonically with γR, is larger. To obtain a larger value of $E_1(\alpha)$, α must be smaller, and hence the time to reach steady state must be shorter. In the example given above for $\theta = \pi/2$, $t_{ss} \approx 8$ min. Thus, by the time steady state is attained in the $\theta = 0$ direction, the plaque has reached its final size.

References

[1] N.K. Jerne and A.A. Nordin, Science 140 (1963) 405.
[2] N.K. Jerne, A.S. Nordin and C. Henry Cell-Bound Antibodies, (ed. B. Amos and H. Koprowski) (Wistar Institute Press, Philadelphia, 1963) p. 109.
[3] N.K. Jerne, C. Henry, A.A. Nordin, H. Fuji, M.C. Koros, Lefkovits, I. Transplant. Rev. 18 (1974) 130.
[4] B. Merchant and B. Peterson J. Immunol. 101 (1968) 860.
[5] G.J.V. Nossal, H. Lewis and N.L. Warner Cell. Immunol. 2 (1971) 13.
[6] A.J. Cunningham Nature 207 (1965) 1106.
[7] A.J. Cunningham, and A. Szenberg, Immunology 14 (1968) 599.
[8] J.S. Ingraham and A. Bussard, J. Exp. Med. 119 (1964) 667.
[9] G.J.V. Nossal and O. Mäkelä, Ann. Rev. Microbiol. 16 (1962) 53.
[10] J.C. Kennedy and M.A. Axelrad, Immunology 20 (1971) 253.
[11] C. DeLisi and G.I. Bell Proc. Nat. Acad. Sci. USA 71 (1974) 16.
[12] C. DeLisi, J. Theoret. Biol. 52 (1975) 419; J. Math. Biol. 2, 317.
[13] B. Goldstein, to be published.
[14] G.J.V. Nossal, A.S. Bussard, H. Lewis and J.C. Mazie, J. Exp. Med. 131 (1970) 894.
[15] G.J.V. Nossal and H. Lewis Immunology 20 (1971) 739.
[16] C.-B. Laurell, Annal. Biochem. 15 (1966) 45.
[17] C.-B. Laurell Scand. J. Clin. Lab. Invest. 29, Suppl. 124 (1972) p. 21.
[18] J.R. Cann (1975) Biophys. Chem. 3 (1975) 206.
[19] J.R. Cann, (1975) Immunochem. 12 (1975) 473.
[20] A.J. Cunningham and S.A. Fordham, Nature 250 (1974) 669.
[21] A.J. Cunningham and L.M. Pilarski, Eur. J. Immunol. 4 (1974) 319.
[22] A.J. Cunningham and L.M. Pilarski, Eur. J. Immunol. 4 (1974) 757.
[23] L.M. Pilarski and A.J. Cunningham, Eur. J. Immunol. 5 (1975) 10.
[24] L.M. Pilarski and A.J. Cunningham, Cunningham, Eur. J. Immunol. 4 (1974) 762.
[25] B. Goldstein, Nature 253 (1975) 637.
[26] C. DeLisi and A. Perelson, J. Theor. Biol. (1976) to be published.
[27] M. Abramowitz and I.A. Stegun, Handbook of Mathematical Functions (National Bureau of Standards, 1964).
[28] V.G. Levich, Physiochemical Hydrodynamics (Prentice Hall, Englewood Cliffs, NJ, 1962).
[29] R.J. Wieme, Agar Gel Electrophoresis (Elsevier, Amsterdam, 1965) p.11.
[30] T. Suzuki and H.F. Deutsch J. Biol. Chem. 242 (1967) 2725.
[31] B. Goldstein and C. DeLisi, Immunochem. 13 (1976) 29.

[32] J.J. Marchalonis and G.J.V. Nossal, Proc. Nat. Acad. Sci. USA 61 (1968) 860.
[33] H.E. Schultz, H. Haupt, K. Heide, G. Möschlin, R. Schmidtberger and G. Schwick, Z. Naturforsch. 176 (1962) 313.
[34] J.H. Humphrey, Nature 216 (1967) 1295.
[35] R. Wurmser and S. Filitti-Wurmser, Progress in Biophysics (eds. J.A.V. Butler and B. Kutz) (Pergamon Press, New York, 1957) p. 87.
[36] N.C. Hughes-Jones, B. Gardner and R. Telford, Biochem. J. 85 (1962) 466.
[37] N.C. Hughes-Jones, B. Gardner and R. Telford, Biochem. J. 88 (1963) 435.
[38] N.C. Hughes-Jones, B. Gardner and R. Telford, Immunology 7 (1964) 72.
[39] C.L. Hornick and F. Karush Immunochem. 9 (1972) 325.
[40] J.L. Fahey and I. Finegold, Cold Spring Harbor Symp. Quant. Biol. 32 (1967) 283.
[41] R.N. Hiramoto, J.R. McGhee and N.M. Hamlin, J. Immunol. 109 (1972) 961.
[42] R.N. Hiramoto, J.R. McGhee and N.M. Hamlin, J. Immunol. 109 (1972) 968.
[43] R.E. Conrad and J.S. Ingraham, J. Immunol. 112 (1974) 17.
[44] B. Goldstein, C. DeLisi and J. Abate, J. Theor. Biol. 52 (1975) 317.
[45] C. DeLisi and B. Goldstein, J. Theoret. Biol. 51 (1974) 313.
[46] C. DeLisi and B. Goldstein, Immunochem. 11 (1974) 661.
[47] H.S. Carslaw and J.C. Jaeger, Conduction of Heat in Solids (Oxford Univ. Press, London, 1959).
[48] S.J. Singer, Ann. Rev. Biochem. 43 (1974) 805.
[49] P.B. Canham and A.C. Burton, Circ. Res. 22 (1968) 405.
[50] A.W. Jay, Biophy. J. 15 (1974) 205.
[51] T.S. Gradshteyn and I.M. Ryzhik, Table of Integrals, Series and Products (Academis Press, New York, 1965).
[52] G.E. Roberts and H.K. Kaufman, Table of Laplace Transforms (Saunders, Philadelphia, 1966).
[53] A.K.C. Wong and W. Sabbadini, J. Immunol. 112 (1974) 2251.